

The critical nature of the Ni spin state in doped NdNiO₂

Mi Jiang,^{1,2} Mona Berciu,^{1,2} and George A. Sawatzky^{1,2}

¹Department of Physics and Astronomy, University of British Columbia, Vancouver B.C. V6T 1Z1, Canada

²Stewart Blusson Quantum Matter Institute, University of British Columbia, Vancouver B.C. V6T 1Z4, Canada

Superconductivity with $T_c \approx 15K$ was recently found in doped NdNiO₂. The Ni¹⁺O₂ layers are expected to be Mott insulators so hole doping should produce Ni²⁺ with $S = 1$, incompatible with robust superconductivity. We show that the NiO₂ layers fall inside a “critical” region where the large pd hybridization favors a singlet ¹A₁ hole-doped state like in CuO₂. However, we find that the superexchange is about one order smaller than in cuprates, thus a magnon “glue” is very unlikely and another mechanism needs to be found.

Introduction: Understanding the mechanism responsible for the appearance of high-temperature superconductivity (SC) in cuprates [1] remains one of the top challenges in condensed matter physics. Despite over 30 years of intense effort that produced numerous proposals, there is no consensus on what is the “pairing glue” [2].

A possible route of breaking this deadlock is to find similar but non-Cu based families of SC, which might help solve the mystery. One of the routes being pursued is to replace Cu²⁺ with Ni¹⁺ in compounds such as LaNiO₂ and NdNiO₂. Both Cu²⁺ and Ni¹⁺ are in the 3d⁹, $S = \frac{1}{2}$ configuration in the parent compound, so the infinite NiO₂ planes appear to be direct counterparts of the CuO₂ planes. After several failed attempts [3–5], SC with T_c of up to 15K was recently found in doped Nd_{0.8}Sr_{0.2}NiO₂ single crystal thin films [6]. This is a very exciting development, suggesting the existence of a Ni-based family of high- T_c SC that may be more like the cuprates than the Fe-based family [7] turned out to be.

To gauge how similar this new SC is to cuprates, we

compare the behaviour of a NiO₂ layer upon doping to that of a CuO₂ layer. Throughout this work, we assume that, like in CuO₂ layers, only the O 2p and the Ni 3d states determine the low-energy physics of the NiO₂ layer, and that stoichiometric NiO₂ layer is a large gap insulator. We note that the nature of the parent compound NdNiO₂ is not yet clear. The thin film in Ref. [6] is metallic, but recent reports found both thin films and bulk crystals that are insulators [8, 9]. As further discussed below, ab-initio studies are also divided; those that find a metallic band, locate it in the Nd layers. If this Nd band exists, charge neutrality demands that electrons present in the Nd layers in the stoichiometric compound, be compensated by holes in the NiO₂ layers, further emphasizing the need to understand the latter subsystem.

For all of these reasons, here we study a NiO₂ layer. A major difference is immediately apparent: NiO₂ should be a Mott insulator [10–13] while the cuprates are charge-transfer insulators, according to the Zaanen-Sawatzky-Allen (ZSA) scheme [14], see sketch in Fig. 1. This is due to a charge transfer energy $\Delta \approx 9$ eV in NiO₂ vs. $\Delta \approx 3$ eV in CuO₂, because the smaller nuclear charge of Ni causes a 5-6eV upward shift of the d¹⁰ state in NiO₂ (the other energy scales, in particular $U_{dd} \approx 6 - 7$ eV, are similar in both types of layers, see below) [15].

Holes doped in a Mott insulating NiO₂ layer would reside on the Ni, not in the O2p band. Because Ni²⁺ (3d⁸) is $S = 1$ in all other known Ni²⁺ oxides, this would make the appearance of rather high- T_c superconductivity very puzzling, and definitely unlike that in cuprates.

In this Letter, we use an impurity calculation including the full Ni:3d⁸ multiplet structure to argue that in fact, NiO₂ lies in the critical crossover region of the ZSA diagram, where the lowest $S = 0$ and $S = 1$ eigenstates cross. It is possible, therefore, that holes doped in NiO₂ layers have a strong O 2p component with the same ¹A₁ symmetry like the Zhang-Rice singlet (ZRS) of cuprates, *i.e.* two holes in orbitals with $x^2 - y^2$ symmetry [16]. This may explain how SC could emerge upon doping of this Mott insulator, as it would make hole doping in NiO₂ rather similar to cuprates. It would also suggest that small changes in the parameters, resulting from variations in lattice parameters through chemical composition

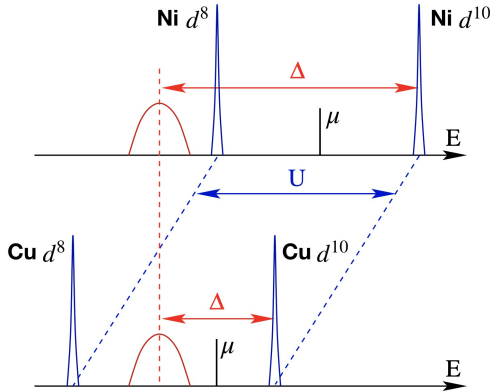


FIG. 1: (color online) Sketch of a Mott insulator (top) vs. a charge transfer insulator (bottom). The narrow (blue) bands are the Hubbard 3d bands while the broader (red) band is the O2p band before the pd hybridization has been switched on. The sketch assumes a similar U but a significantly larger Δ , like for NdNiO₂ as compared to LaCuO₄. Below (above) the chemical potential μ are the electron removal (addition) states, if the starting configuration is Ni/Cu 3d⁹ plus a full O 2p band.

or applied pressure, could also stabilize the more common 3B_1 lowest energy hole state, *i.e.* one hole in $x^2 - y^2$ and the other in $3z^2 - r^2$ symmetry. This is a testable prediction, which may be linked to the lack of SC in the closely related LaNiO_2 compound [6]. It is also consistent with the reported differences in the properties of thin films and bulk crystals grown in different labs, and their high sensitivity to applied pressure.

While a 1A_1 , ZRS-like type of hole-doped state would make NiO_2 similar to CuO_2 , it does not automatically confirm a similar SC like in cuprates. This is because another consequence of the larger Δ is that the superexchange [17]:

$$J_{dd} = \frac{4t_{pd}^4}{\Delta^2 U_{dd}} + \frac{8t_{pd}^4}{\Delta^2 (U_{pp} + 2\Delta)}$$

must be around ten times smaller in NiO_2 than in cuprates [11]. While this explains the lack of antiferromagnetic (AFM) order in the parent compound [4, 5], it also makes it very unlikely that SC in the new material is mediated through magnon-exchange. Insofar as that is a leading scenario for cuprate SC, this means either that the new SC has a different mechanism than cuprates, or that SC in cuprates is not (primarily) magnon-mediated. We further discuss these implications below.

Model: We study a hole doped into a system consisting of a Ni^{1+} ($3d^9$) impurity properly embedded in an infinite square lattice of $\text{O}2p^6$ ions. The Hamiltonian is:

$$\mathcal{H} = \hat{U}_{dd} + \hat{T}_{pd} + \hat{T}_{pp} + \hat{\Delta} + \hat{U}_{pp}. \quad (1)$$

Here, \hat{U}_{dd} includes all Coulomb and exchange integrals of the $3d^8$ multiplet, which determine the spin and symmetry of the lowest-energy hole addition state. Matrix elements between the $3d$ orbitals $b_1(d_{x^2-y^2})$, $a_1(d_{3z^2-r^2})$, $b_2(d_{xy})$, $e_x(d_{xz})$ and $e_y(d_{yz})$ are in terms of the Racah parameters A, B, C [18]. The $3d$ orbitals are assumed to be degenerate, *i.e.* we omit point-charge crystal splittings. (This is a good approximation because it is the hybridization with the O orbitals, included in our model, that accounts for most of the difference between the effective on-site energies of the $3d$ levels). \hat{T}_{pd} and \hat{T}_{pp} describe hopping of holes between the $\text{Ni}3d$ orbitals and adjacent $\text{O}2p$ ligand orbitals, and between nearest neighbour O ligand orbitals, respectively. We note that we have checked explicitly that including the second pair of in-plane, π -type $\text{O}2p$ orbitals has essentially no effect on the results reported below. Finally, $\hat{\Delta}$ measures the difference in the on-site energies of $3d$ and $2p$ orbitals, as measured from the full O $2p$ band to the Ni d^{10} state, while \hat{U}_{pp} is an on-site Hubbard repulsion when two holes are in the same O ligand orbital.

We study the GS of this impurity system with either one hole (undoped) or two holes (doped) using Exact Diagonalization. We recently used this model to study a Cu^{2+} impurity embedded in a square O lattice [19];

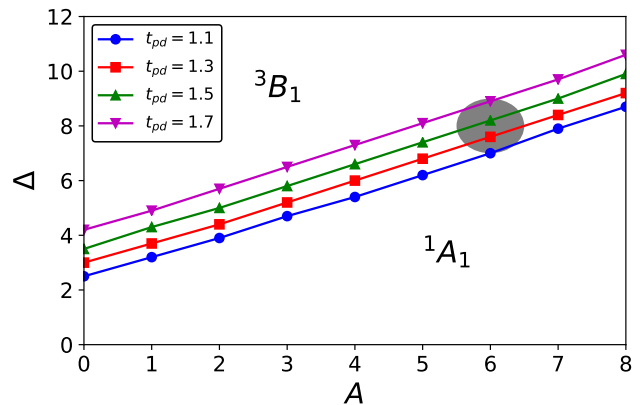


FIG. 2: (color online) Phase diagram for the stability of a 3B_1 triplet ground-state, expected for a doped Mott insulator, *vs.* a 1A_1 singlet ground-state like in hole-doped cuprates, for different values of Δ and A , measured in eV. Other parameters are $t_{pp} = 0.55\text{eV}$, $B = 0.15\text{eV}$, $C = 0.58\text{eV}$, $U_{pp} = 0$. The four lines correspond to $t_{pd} = 1.1, 1.3, 1.5$ and 1.7eV . We expect NdNiO_2 to lie in the shaded region.

we refer the reader there for further details, in particular why the proper modelling of the O sublattice is essential.[20] We use fits to ab-initio results [21–23] to extract the hybridization between the Ni impurity and neighbor O, $t_{pd} \approx 1.3 - 1.5\text{eV}$, and between adjacent O, $t_{pp} \approx 0.55\text{eV}$. These values are similar to those in the cuprates. For t_{pd} , this is because of a partial cancellation of changes due to the somewhat larger lattice constant of the nickelates, and to the larger orbital radius of their d orbital, due to the smaller nuclear charge. For t_{pp} , this is because the lattice constant increase is not that significant. We keep the same values for the Racah parameters B, C , because they are set by atomic physics and not much influenced by screening effects, as verified experimentally in other systems with Ni^{2+} ions [15]. U_{pp} plays little role for the results discussed below, so we set it $U_{pp} = 0$ (very similar results are obtained for $U_{pp} \approx 3\text{eV}$, however). As already mentioned, we expect the on-site Coulomb repulsion on the Ni^{1+} to be comparable to that on the Cu^{2+} , $U_{dd} = A + 8B + 3C \approx 6 - 7\text{eV}$, while the charge transfer $\Delta \approx 7 - 9\text{eV}$ as opposed to $\Delta \approx 3\text{eV}$ in cuprates [24].

Results: Figure 2 shows the one-hole phase diagram as a function of A and Δ . It consists of two regions with ground-states (GS) of 1A_1 and 3B_1 symmetry [19, 25, 26], respectively. In the 3B_1 region the doped hole primarily sits on the Ni and locks into a triplet with the other hole, by Hund’s exchange. More specifically (also see below), one hole occupies a wavefunction with dominant $3d_{x^2-y^2}$ character plus a small contribution from the $x^2 - y^2$ linear combination of adjacent $\text{O}2p$ orbitals, while the second hole occupies the $3z^2 - r^2$ counterpart. In contrast, in the 1A_1 region the doped hole occupies primarily the $x^2 - y^2$

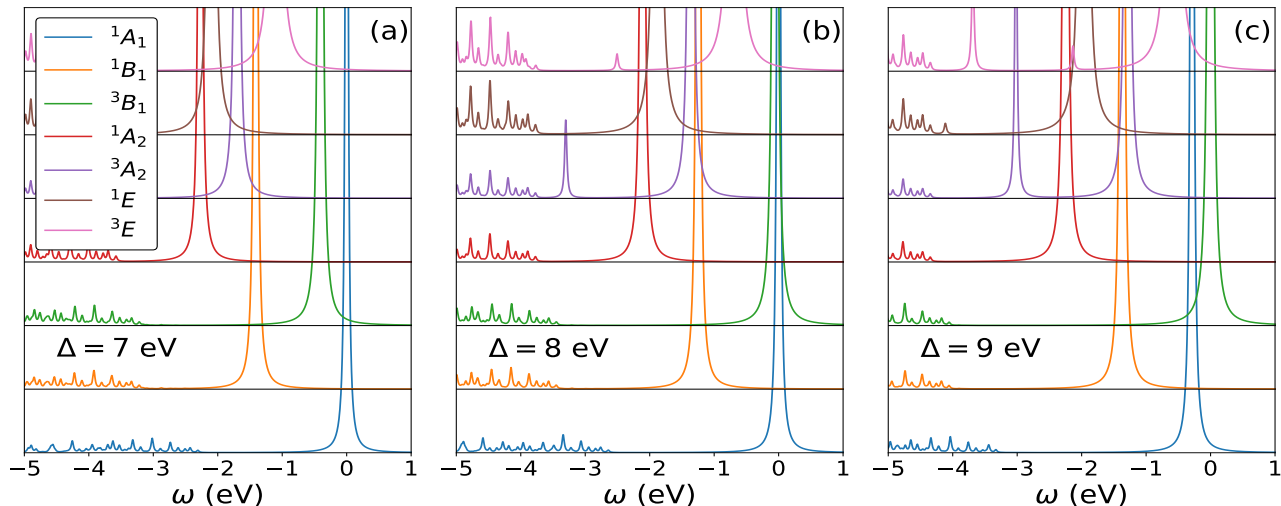


FIG. 3: (color online) Spectral weight for addition of a doped hole, when $t_{pd} = 1.5\text{eV}$ and $A = 6.0\text{eV}$ are kept constant, while $\Delta = 7, 8, 9\text{eV}$ in the left, central and right panels, respectively. Spectra are shifted such that the ground-state is located at zero energy. With increasing Δ , its character changes from 1A_1 (spectrum shown by the blue, lowest curve) to 3B_1 (spectrum shown by the green, 3rd lowest curve).

“molecular”-like $O2p$ orbital with a small admixture of the $3d_{x^2-y^2}$ orbital, and is locked in a singlet with the other hole which has primarily $3d_{x^2-y^2}$ character.

The three lines show how the boundary shifts with t_{pd} , and the shaded ellipse is the area we believe to be relevant for the NiO_2 layer. Clearly, it falls in the borderline regime where the ground-state changes its nature.

To better understand what happens, and how it is possible for the doped states of a Mott insulator to instead look more like those of a charge-transfer insulator, we plot in Fig. 3 spectral densities for the addition of the doped hole, resolved by point symmetry. The three panels correspond to $\Delta = 7, 8, 9\text{eV}$ while $t_{pd} = 1.5\text{eV}$ and $A = 6.0\text{eV}$. They show that with increasing Δ , the ground-state transitions from having 1A_1 symmetry to having the 3B_1 symmetry expected in the large Δ limit. (The same transition is seen varying t_{pd} for a fixed Δ .)

With increasing Δ , we see an increasing separation between the discrete peaks showing the low-energy states with the doped hole bound to the impurity Ni with various symmetries (these include the ground-state, always shifted to occur at zero energy), and the continuum which describes excited states with the doped hole moving freely in the O band. (The band is a sequence of closely spaced peaks because for computational convenience, we limit the size of the O lattice to be 20×20 . In the thermodynamic limit, this consequence of confinement to a “finite-box” disappears and the continuum becomes smooth, but its band-edges do not move).

Physically, what happens is that when the separation between the $3d^8$ peak (which depends on the symmetry

and the spin of the state) and the O band sketched in Fig. 1 is smaller or comparable with t_{pd} , their hybridization is responsible for the appearance of these low-energy bound states in all the channels; in particular, the one with 1A_1 symmetry as the ground-state. As Δ increases and the distance between the two features becomes larger than t_{pd} , the ground-state switches to the expected 3B_1 character for a Mott insulator, which is the conventional Hund’s rule ground state for $\text{Ni } d^8$.

In Figure 4 we show the evolution of the ground state weights of the various components with increasing Δ , for $t_{pd} = 1.5\text{eV}$ and $A = 6\text{eV}$. These components of the two-hole wavefunction are products of the single particle states of various symmetries. Included in this analysis are all the d^8 , d^9L and $d^{10}L^2$ states. The weights of the states involving the hole continua are summed over energy.

We see that the only d^8 basis states with reasonable weights are the a_1a_1, b_1b_1 , and a_1b_1 states (we use the standard notation $a_1 \equiv d_{3z^2-r^2}, b_1 \equiv d_{x^2-y^2}$ [19, 26]). These are also the only symmetries that are important for the d^9L and $d^{10}L^2$ continuum states. We see that for $\Delta < A$, *i.e.* in the charge transfer gap region, the amount of total d^8 character is small, increasing as we approach the transition to the 3B_1 ground state. Simultaneously, the amount of $d^{10}L^2$ is gradually decreasing because the separation between the $d^{10}L^2$ and the d^9L continua is increasing as Δ increases. The transition occurs at $\Delta = 8.1\text{eV}$, which is considerably higher than where the transition from the Mott to the charge transfer insulator occurs in the ZSA diagram. This is because the L_{b_1} symmetry states in the O 2p band are located at the

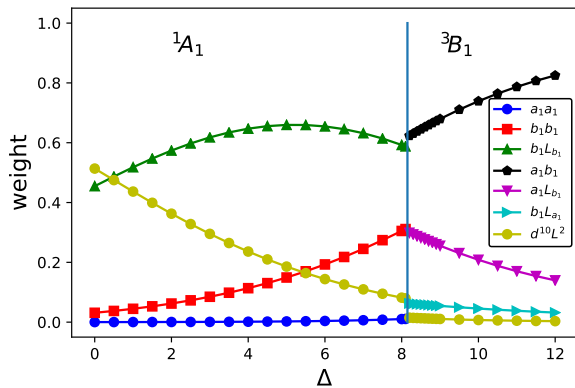


FIG. 4: (color online) Variation of the ground state weights of the dominant components versus Δ , for fixed $t_{pd} = 1.5$ eV, $A = 6.0$ eV. Note that the dominant component changes dramatically as the ground state switches from 1A_1 to 3B_1 . The vertical line denotes the critical value $\Delta = 8.1$ eV separating the two phases.

top of the O band and not at its center, so their effective Δ is about 1.5 eV lower. Note the abrupt change in the weights of the d^8 components, especially the a_1b_1 component, as we enter the region where the ground-state is 3B_1 . Here, $d^8(a_1b_1)$ is the dominant component, unlike the ZRS-like $d^9(b_1)L_{b_1}$ dominating the 1A_1 symmetry.

These results suggest that the minimal model able to describe both phases is the counterpart of Eq. (1) that includes only the e_g orbitals (not all five Ni 3d orbitals). Simpler minimal models are available to describe each phase. On the 1A_1 side, one can project down to a single band Hubbard-like or t - J -like model [16], although it is controversial whether the O orbitals should be integrated out [27–29]. On the 3B_1 side, a so-called type-II t - J model has been recently proposed to describe the motion of a hole with spin $S = 1$ in a background of spin- $\frac{1}{2}$ [30]; older work along similar lines was reported in Ref. [31].

Summary and discussion: To conclude, we performed an impurity calculation to demonstrate that despite nominally being in the Mott region of the ZSA scheme, in fact a NiO₂ layer falls inside a critical region of the parameter space where the strong pd hybridization may favor a $S = 0$ hole-doped state with 1A_1 symmetry, similar to the cuprates. However, the triplet 3B_1 state is close in energy so that small changes in the parameters resulting from changes in the lattice structure with chemical substitution, with epitaxial strain or with pressure could stabilize the triplet state, making SC unlikely.

We also pointed out that these NiO₂ layers have large charge transfer energies Δ , leading to a superexchange around an order of magnitude smaller than in cuprates. This fact severely challenges the scenario of spin fluctuations as the glue for superconductivity here, although that is currently the prevalent scenario in cuprates.

Before realistic proposals for the mechanism of superconductivity can be put forward, it is imperative to know whether metallic bands appear in the Nd layer. As mentioned, reports both of metallic and of insulating stoichiometric samples exist in the literature. Ab-initio studies are also divided. Some suggest that the parent compound is a metal with a Nd band crossing the Fermi energy [11, 23, 32–40], but this becomes gapped if correlations are included in a LDA+U approach [21], and/or upon various chemical substitutions [21, 22]. In any event, if metallicity due to bands located in the other layers is confirmed, it will certainly be necessary to understand their interplay with the NiO₂ layers. This would make superconductivity in the new compound definitely unlike that of cuprates, and would suggest the fascinating possibility of another mechanism that stabilizes high- T_c superconductivity. While such work has already begun, see for *e.g.* Refs. [10, 30, 41–53], it is essential to first have a good understanding of the individual behaviour of either kind of layer with doping. The work presented here demonstrates that the NiO₂ layers should not be treated like simple Mott insulators or charge transfer insulators.

Acknowledgements: This work was funded by the Stewart Blusson Quantum Matter Institute at University of British Columbia, and by the Natural Sciences and Engineering Research Council of Canada.

-
- [1] J. G. Bednorz and K. A. Müller, *Zeitschrift für Physik B Condensed Matter* **64**, 189 (1986), URL <https://doi.org/10.1007/BF01303701>.
 - [2] P. W. Anderson, *Science* **316**, 1705 (2007), ISSN 0036-8075, URL <http://science.sciencemag.org/content/316/5832/1705>.
 - [3] M. Crespin, P. Levitz and L. J. Gattineau, *Chem. Soc. Faraday Trans.* **2** **79**, 1181-1194 (1983), URL <https://pubs.rsc.org/en/content/articlelanding/1983/F2/F29837901181#!divAbstract>.
 - [4] M. A. Hayward, M. A. Green, M. J. Rosseinsky and J. J. Sloan, *J. Am. Chem. Soc.* **121**, 8843-8854 (1999), URL <https://pubs.acs.org/doi/10.1021/ja991573i>.
 - [5] M. A. Hayward and M. J. Rosseinsky, *Solid State Sci.* **5**, 839-850 (2003), URL <https://www.sciencedirect.com/science/article/pii/S1293255803001110>.
 - [6] Li, D. et al., *Nature* **572**, 624-627 (2019), URL <https://www.nature.com/articles/s41586-019-1496-5>.
 - [7] Y. Kamihara et al., *J. Am. Chem. Soc.* **128(31)**, 10012 (2006), URL <https://pubs.acs.org/doi/10.1021/ja063355c>.
 - [8] X. Zhou et al., *Rare Metals* **39**, 368-374 (2020), URL <https://link.springer.com/article/10.1007/s12598-020-01389-2>.
 - [9] Q. Li et al., *Communications Materials* **1**, 16 (2020), URL <https://www.nature.com/articles/s43246-020-0018-1>.
 - [10] M. Hepting et al., *Nat. Materials* **19**, 381 (2020), URL <https://www.nature.com/articles/s41563-019-0585-z>.

- [11] Z. Liu et al., arXiv:1912.01332, URL <https://arxiv.org/abs/1912.01332v2>.
- [12] Y. Nomura et al., Phys. Rev. B **100**, 205138 (2019), URL <https://journals.aps.org/prb/abstract/10.1103/PhysRevB.100.205138>.
- [13] F. Bernardini et al., arXiv:1911.11788, URL <https://arxiv.org/abs/1911.11788>.
- [14] J. Zaanen, G. A. Sawatzky and J. W. Allen, Phys. Rev. Lett. **55**, 418 (1985), URL <https://journals.aps.org/prl/abstract/10.1103/PhysRevLett.55.418>.
- [15] J. Zaanen and G. A. Sawatzky, Journal of Solid State Chemistry **88**, 8-27 (1990), URL <https://www.sciencedirect.com/science/article/pii/0022459690902029>.
- [16] F. C. Zhang and T. M. Rice, Phys. Rev. B **37**, 3759 (1988), URL <https://link.aps.org/doi/10.1103/PhysRevB.37.3759>.
- [17] J. Zaanen and G. A. Sawatzky, Canadian Journal of Physics **65(10)**, 1262-1271 (1987), URL <https://www.nrcresearchpress.com/doi/abs/10.1139/p87-201#.XWVPPxew5k>.
- [18] M. E. Rose, Elementary Theory of Angular Momentum, Dover Publications (2011).
- [19] M. Jiang, M. Moeller, M. Berciu and G. A. Sawatzky, Phys. Rev. B **101**, 035151, URL <https://journals.aps.org/prb/abstract/10.1103/PhysRevB.101.035151>.
- [20] Note that the relevant energy scale is the bandwidth $8t_{pp} \approx 4.5$ eV. This is a considerable energy, which is why the proper modelling of the O band is important.
- [21] K. Foyevtsova, I. Elfimov and G. A. Sawatzky, to be published.
- [22] L. Si et al., Phys. Rev. Lett. **124**, 166402 (2020), URL <https://journals.aps.org/prl/abstract/10.1103/PhysRevLett.124.166402>.
- [23] J. Karp et al., arXiv:2001.06441, URL <https://arxiv.org/abs/2001.06441>.
- [24] M. S. Hybertsen, M. Schlter and N. E. Christensen, Phys. Rev. B **39**, 9028 (1989), URL <https://journals.aps.org/prb/abstract/10.1103/PhysRevB.39.9028>.
- [25] C.J. Ballhausen, Introduction to ligand field theory, McGraw-Hill series in advanced chemistry (1962).
- [26] H. Eskes and G. A. Sawatzky, Phys. Rev. Lett. **61**, 1415 (1988), URL <https://link.aps.org/doi/10.1103/PhysRevLett.61.1415>.
- [27] B. Lau, M. Berciu, and G. A. Sawatzky, Phys. Rev. Lett. **106**, 036401 (2011), URL <https://journals.aps.org/prl/abstract/10.1103/PhysRevLett.106.036401>.
- [28] H. Ebrahimnejad, G. A. Sawatzky and M. Berciu, Nature Physics **10**, 951-955 (2014), URL <https://www.nature.com/articles/nphys3130>.
- [29] H. Ebrahimnejad, G. A. Sawatzky and M. Berciu, J. Phys: Cond. Matt. **28**, 105603 (2016), URL <https://iopscience.iop.org/article/10.1088/0953-8984/28/10/105603>.
- [30] Y.-H. Zhang and A. Vishwanath, Phys. Rev. Res. **2**, 023112 (2020), URL <https://journals.aps.org/prresearch/abstract/10.1103/PhysRevResearch.2.023112>.
- [31] J. Zaanen, A. M. Oles and P. Horsch, Phys. Rev. B **46**, 5798(R) (1992), URL <https://journals.aps.org/prb/abstract/10.1103/PhysRevB.46.5798>.
- [32] K.-W. Lee and W. E. Pickett, Phys. Rev. B **70**, 165109 (2004), URL <https://journals.aps.org/prb/abstract/10.1103/PhysRevB.70.165109>.
- [33] A.-S. Botana and M. R. Norman, Phys. Rev. X **10**, 011024 (2020), URL <https://journals.aps.org/prx/abstract/10.1103/PhysRevX.10.011024>.
- [34] H. Sakakibara et al., arXiv:1909.00060v2, URL <https://arxiv.org/abs/1909.00060v2>.
- [35] J. Gao et al., arXiv:1909.04657, URL <https://arxiv.org/abs/1909.04657>.
- [36] S. Rye et al., Phys. Rev. B **101**, 064513 (2020), URL <https://dx.doi.org/10.1103/PhysRevB.101.064513>.
- [37] P. Jiang et al., Phys. Rev. B **100**, 201106 (2019), URL <https://journals.aps.org/prb/abstract/10.1103/PhysRevB.100.201106>.
- [38] M. Hirayama et al., Phys. Rev. B **101**, 075107 (2020), URL <https://dx.doi.org/10.1103/PhysRevB.101.075107>.
- [39] Y. Gu et al., arXiv:1911.00814, URL <https://arxiv.org/abs/1911.00814>.
- [40] F. Lechermann, Phys. Rev. B **101**, 081110 (2020), URL <https://dx.doi.org/10.1103/PhysRevB.101.081110>.
- [41] X. Wu et al., Phys. Rev. B **101**, 060504 (2020), URL <https://dx.doi.org/10.1103/PhysRevB.101.060504>.
- [42] H. Zhang et al., Phys. Rev. Research **2**, 013214 (2020), URL <https://journals.aps.org/prresearch/abstract/10.1103/PhysRevResearch.2.013214>.
- [43] G. Zhang et al., Phys. Rev. B **101**, 020501 (2020), URL <https://journals.aps.org/prb/abstract/10.1103/PhysRevB.101.020501>.
- [44] J. E. Hirsch and F. Marsiglio, Physica C: Superconductivity **566**, 1353534 (2019), URL <https://www.sciencedirect.com/science/article/pii/S0921453419303053>.
- [45] P. Werner and S. Hoshino, Phys. Rev. B **101**, 041104 (2020), URL <https://journals.aps.org/prb/abstract/10.1103/PhysRevB.101.041104>.
- [46] L. Hu and C. Wu, Phys. Rev. Research **1**, 032046 (2019), URL <https://journals.aps.org/prresearch/abstract/10.1103/PhysRevResearch.1.032046>.
- [47] F. Bernardini, V. Olevano and A. Cano, Phys. Rev. Research **2**, 013219 (2020), URL <https://journals.aps.org/prresearch/abstract/10.1103/PhysRevResearch.2.013219>.
- [48] Y. Fu et al., arXiv:1911.03177, URL <https://arxiv.org/abs/1911.03177>.
- [49] M. Choi, K. Lee and W. E. Pickett, Phys. Rev. B **101**, 020503 (2020), URL <https://journals.aps.org/prb/abstract/10.1103/PhysRevB.101.020503>.
- [50] J. Chang, J. Zhao and Y. Ding, arXiv:1911.12731, URL <https://arxiv.org/abs/1911.12731v1>.
- [51] E. F. Talantsev, arXiv:1912.06099, URL <https://arxiv.org/abs/1912.06099>.
- [52] M. Kitatani et al., arXiv:2002.12230, URL <https://arxiv.org/abs/2002.12230>.
- [53] E. Been et al., arXiv:2002.12300, URL <https://arxiv.org/abs/2002.12300>.